

CHEMISTRY

A **European** Journal

Supporting Information

Triplet–Triplet Annihilation Upconversion in a MOF with Acceptor-Filled Channels

Shadab Gharaati^{+, [a]} Cui Wang^{+, [b, c]} Christoph Förster,^[a] Florian Weigert,^[b]
Ute Resch-Genger,^{*[b]} and Katja Heinze^{*[a]}

chem_201904945_sm_miscellaneous_information.pdf
chem_201904945_sm_TTA-MOF_video.mp4
chem_201904945_sm_TTA_MOF_video.mp4

Supporting Information

Table of Contents

1. Chemicals and Instrumentation

2. Syntheses

- a) Synthesis of Pd(TCPP).
- b) Synthesis of PCN-222(Pd).
- c) Synthesis of DPA-F₁₄@PCN-222(Pd).
- d) Synthesis of CA@PCN-222(Pd).
- e) Synthesis of CA/DPA@PCN-222(Pd).
- f) Release of DPA from CA/DPA@PCN-222(Pd) in toluene.
- g) Release of DPA from CA/DPA@PCN-222(Pd) in water.

3. Spectroscopic Data

Figure S0. ¹³C{¹H} NMR spectrum of Pd(TCPP) in DMSO-d₆.

Figure S1. UV/Vis absorption and emission spectra of PCN-222(Pd).

Figure S2. IR spectrum of PCN-222(Pd).

Figure S3. ¹⁹F NMR spectrum of DPA-F₁₄ in CD₂Cl₂.

Figure S4. ¹⁹F MAS NMR spectrum of DPA-F₁₄.

Figure S5. ¹⁹F MAS NMR spectrum of DPA-F₁₄@PCN-222(Pd).

Figure S6. UV/Vis absorption and emission spectra of DPA in toluene and emission spectrum of DPA.

Figure S7. Experimental PXRD pattern of PCN-222(Pd) and CA/DPA@PCN-222(Pd) and simulated PXRD pattern of PCN-222(Pd).

Figure S8. IR spectra of CA@PCN-222(Pd) and CA/DPA@PCN-222(Pd).

Figure S9. UV/Vis absorption spectra of PCN-222(Pd) and CA/DPA@PCN-222(Pd).

Figure S10. Stability of PCN-222(Pd) under laser irradiation in the presence of tiny amounts of O₂.

Figure S11. Stability of CA/DPA@PCN-222(Pd) under laser irradiation in the absence of O₂.

Figure S12. Fluorescence decay of DPA with $\lambda_{exc} = 410$ nm.

Figure S13. Fluorescence decay of DPA with $\lambda_{exc} = 405$ nm.

Figure S14. Luminescence decay of the DPA acceptor in CA/DPA@PCN-222(Pd).

Figure S15. Luminescence decay of PCN-222(Pd) with $\lambda_{exc} = 524$ nm.

Figure S16. Luminescence decay of the donor in CA/DPA@PCN-222(Pd) with $\lambda_{exc} = 524$ nm.

Figure S17. UCL emission of CA/DPA-PCN-222(Pd) under O₂-free conditions and in the presence of O₂.

Figure S18. Emission spectra of PCN-222(Pd) and UCL emission of CA/DPA-PCN-222(Pd) at three different points of the same sample.

Figure S19. Optical photographs of CA/DPA-PCN-222(Pd).

Figure S20. UCL emission of acceptor@PCN-222(Pd) with acceptor = 2,5,8,11-tetra-*tert*-butylperylene.

4. References

1. Chemicals and Instrumentation

Solvents were used as received from commercial suppliers (Acros Organics, Alfa Aesar, Fischer Scientific and Sigma-Aldrich). 1,2,3,4,5,6,7,8-Octafluoro-9,10-bis[4-(trifluoromethyl)phenyl]anthracene DPA-F₁₄, 9,10-diphenylanthracene DPA, ZrCl₄, 2,5,8,11-tetra-*tert*-butylperylene, oleic acid and caprylic acid CA were obtained from Sigma-Aldrich. A universal oven UF55plus (Mettler, Germany) was employed for MOF synthesis. NMR spectra were measured on a Bruker Avance DRX 400 spectrometer at 400.31 MHz (¹H), 100.67 MHz (¹³C) and 376.66 MHz (¹⁹F). ¹⁹F MAS NMR experiments were conducted on a Bruker 400 DSX NMR spectrometer equipped with a 2.5 mm 2 channel probe head at 376.25 MHz ¹⁹F frequency at 20 kHz magic angle spinning averaging between 128 and 1024 transients for the different experiments with a delay of 5 sec. IR spectra were recorded with a Bruker ALPHA II FT-IR spectrometer with a Platinum Di-ATR module. UV/Vis/near-IR spectra for uptake and release experiments were recorded on a Varian Cary 5000 spectrometer using 1.0 cm cells (Hellma, Suprasil).

In order to exclude oxygen, the MOFs were modified with the annihilator and the solvent under rigorous exclusion of oxygen. The TTA-UC samples were placed between two glass slides sealed with epoxy glue and these were sealed in a screw cap cuvette in a glove box (<10 ppm O₂).

TTA-UCL spectra were recorded with an Edinburgh Instruments spectrometer (FLS 920) equipped with a 532 nm cw laser (5.9 mW). A 495 nm short pass filter was placed between the laser source and the sample holder to avoid direct excitation of DPA. Two 532 nm notch filters were placed between the sample holder and the detector to suppress the excitation signal observed on the detector, when complete emission spectra in the range of 400–850 nm were measured. For excitation power dependent TTA-UC measurements, the laser power was varied with a tunable OD filter. The excitation power density was calculated from the excitation power divided by the laser spot size on the sample. The excitation power was determined with a power meter (Newport 841-PE Powermeter), under the consideration that reflections on the glass surfaces cause ca. 11% laser power losses as determined separately with five measurements at different excitation power. The darkened spot on the sample, which was caused by ¹O₂ bleaching, was taken as the effective laser spot irradiated on the sample. The spot size was determined under a microscope with help of a micrometer glass scale.

Luminescence decay of DPA under direct excitation of 410 nm at 9.7 MHz was obtained with the FLS 920, yet in this case using a supercontinuum laser (NKT FIU 15) as excitation source and a microchannel plate photomultiplier tube (MCP-PMT; R3809U50). Luminescence decay of the sensitizer in CA/DPA@PCN-222(Pd) was determined under 524 nm excitation at 100 Hz on the spectrofluorometer FSP 920 from Edinburgh Instruments, using a μ s xenon flashlamp and multi-channel scaling mode. For time resolved measurements at excitation power densities above the saturation threshold an inverted confocal laser scanning microscope was also used. A semi-apochromat water immersion objective with a large working distance (60 \times , NA 1.0 by Olympus) focused the excitation light onto a very small spot of the sample through the glass encapsulation, while working under continuous argon flow. Measurement of the decay kinetics of the sample was done by time correlated single photon counting (TCSPC) of the emission signal employing a single photon sensitive avalanche photodiode (SPADs, from MPD) for detection. DPA decay measurements were carried out under direct excitation

at 405 nm using a fixed wavelength diode laser pulsed at 5 MHz and a dichroic mirror (435 nm long pass) to suppress the contribution of the excitation light. Excitation for TTA-UC decay measurements was carried out with a PicoQuant Solea supercontinuum laser set at an emission wavelength of 524 nm (15 nm bandwidth). Pulsed excitation was realized by mechanical modulation of the emission signal with a chopper wheel set at a frequency of 100 Hz. For TTA-UC decay measurements (440 nm) a dichroic mirror (500 nm short pass) and an additional short pass filter (500 nm) were used, while for the measurement of the MOF sensitizer decay (in the absence of the annihilator) (690 nm) a dichroic mirror (600 nm long pass) and an additional long pass filter (650 nm) have been used to minimize the background signal by suppressing contributions from the excitation light and other emission bands.

Cell parameter determination from single crystal intensity data were collected with a STOE IPDS-2T diffractometer with an Oxford cooling system using Mo- K_{α} radiation at 120 K. Diffraction frames were integrated and most were corrected for absorption using the STOE X-Red software package.¹ Powder X-ray diffraction (PXRD) was carried out with a STOE STADI P powder diffractometer equipped with a Ge(111) monochromator using Cu- $K_{\alpha 1}$ radiation at 40 kV and 30 mA. Intensities were collected by a linear position sensitive detector (lin PSD, STOE, Kr/CH₄). XRD data were simulated using Mercury 3.5.1 (Build RC5).² Elemental analyses were conducted by the microanalytical laboratory of the chemical institutes of the University of Mainz.

2. Syntheses

a) Synthesis of Pd(TCPP)

Meso-tetrakis[4-(methoxycarbonyl)phenyl]porphyrin, H₂TMCPP, was synthesized with slight modifications of established procedures.³ Methyl 4-formylbenzoate (5 g, 30 mmol) was dissolved in propionic acid (72.5 ml). Freshly distilled pyrrol (2.11 ml, 30 mmol) was added dropwise. The mixture was heated to reflux for 15 h under an argon atmosphere. After cooling to room temperature, methanol (50 ml) was added. The purple precipitate was collected by filtration and washed with methanol, ethyl acetate and THF. Yield: 1.2 g (1.42 mmol, 18.9%). ¹H NMR (THF-d₈, 400 MHz): δ = 8.84 (s, 8H), 8.45 (d, ³J_{HH} = 8 Hz, 8H), 8.33 (d, ³J_{HH} = 8 Hz, 8H), 4.05 (s, 12H), -2.77 (s, 2H) ppm. FT-IR: $\tilde{\nu}$ = 3317, 2942, 1721, 1604, 1433, 1271, 1098, 1020, 962, 861, 804, 760, 736, 703 cm⁻¹. UV/Vis (CH₂Cl₂): λ_{max} = 420 (ϵ = 495550 M⁻¹ cm⁻¹, Soret band), 516, 549, 590, 647 nm (Q bands).

(*Meso*-tetrakis[4-(methoxycarbonyl)phenyl]porphyrinato)palladium(II), Pd(TMCP), was synthesized with slight modifications of established procedures for palladium porphyrins.⁴ H₂TMCP (100 mg, 0.118 mmol) and palladium acetate (53 mg, 0.236 mmol) were refluxed in benzonitrile (10 ml) for 1 h. Repeated recrystallization and precipitation from DMF/H₂O solutions gave Pd(TMCP). Yield: 90 mg (0.0995 mmol, 84.3%). ¹H NMR (CDCl₃, 400 MHz): δ = 8.78 (s, 8H), 8.43 (d, ³J_{HH} = 8 Hz, 8H), 8.23 (d, ³J_{HH} = 8 Hz, 8H), 4.11 (s, 12H) ppm. FT-IR: $\tilde{\nu}$ = 2951, 2921, 1719, 1606, 1433, 1272, 1175, 962, 822, 806, 762 cm⁻¹. UV/Vis (toluene): λ_{max} = 419 (ϵ = 252915 M⁻¹ cm⁻¹, Soret band), 524, 555 nm (Q bands).

(*Meso*-tetrakis(4-carboxyphenyl)porphyrinato)palladium(II), Pd(TCP), was prepared from Pd(TMCP) (750 mg, 0.788 mmol) dissolved in a mixture of THF (25 ml) and MeOH (25 ml). A solution of KOH (2.63 g, 46.95 mmol) in H₂O (25 ml) was added to the mixture. After refluxing overnight and cooling to room temperature, the solvents were removed under reduced pressure. The residue was dissolved in hot water (80°C) until the solid fully dissolved. The solution was acidified with 1 M HCl until no further precipitate was detected. The brown solid was filtered, washed with water and dried under reduced pressure. Yield: 650 mg (0.726 mmol, 92.1%). ¹H NMR (THF-d₈, 400 MHz): δ = 11.64 (s, 4H), 8.82 (s, 8H), 8.44 (d, ³J_{HH} = 8 Hz, 8H), 8.27 (d, ³J_{HH} = 8 Hz, 8H) ppm. ¹³C{¹H} NMR (DMSO-d₆, 100 MHz): δ = 167.6, 145.1, 140.7, 134.2, 131.7, 130.9, 128.1, 121.2 ppm. FT-IR: $\tilde{\nu}$ = 2922, 2852, 1683, 1603, 1400, 1259, 1080, 1010, 791, 766, 707 cm⁻¹. UV/Vis (DMF): λ_{max} = 419 (ϵ = 604320 M⁻¹ cm⁻¹, Soret band), 525 and 555 nm (Q bands). Phosphorescence (DMF): λ = 609, 692 nm.

b) Synthesis of PCN-222(Pd)

PCN-222(Pd) was synthesized analogous to the preparation of PCN-222(M) with slight modifications.⁵ ZrCl₄ (35 mg, 0.15 mmol) was ultrasonically dissolved in *N,N*-diethylformamide (4 ml) for 30 min in a 10 ml Pyrex vial. Pd(TCPP) (25 mg, 0.028 mmol) was added and dissolved by ultrasonication for 10 min. Benzoic acid (1350 mg, 11 mmol) was added and ultrasonically dissolved for 30 min. The mixture was heated to 120°C (oven temperature) for 48 h and then at 135°C (oven temperature) for 24 h. After cooling down to room temperature, the precipitate was collected by filtration. The dark red-brown, needle shaped crystals were washed with DMF (2×10 ml) and acetone (2×10 ml). The crystals were covered with acetone (5 ml), allowed to stand for 12 h and collected by filtration. Yield 25 mg (0.019 mmol, 69%). FT-IR: $\tilde{\nu}$ = 3065, 2966, 1698, 1597, 1550, 1410, 1350, 1307, 1179, 1013, 795, 775, 723, 710, 684, 665, 461 cm⁻¹. Anal. calcd. for C₄₈H₃₂N₄O₁₆PdZr₃ (1300.88): C, 44.32; H, 2.48; N, 4.31 %. Found: C, 47.45; H, 1.66; N, 4.44 %. Cell constants: $a = b = 42.455(7)$ Å, $c = 17.1037(2)$ Å, $\alpha = \beta = 90^\circ$, $\gamma = 120^\circ$.

c) Synthesis of DPA-F₁₄@PCN-222(Pd)

After the removal of acetone by filtration, PCN-222(Pd) (20 mg, ca. 0.015 mmol) was dried under reduced pressure for 12 h at 60°C. Under an inert atmosphere, a solution of DPA-F₁₄ (200 mg, 0.33 mmol) in dry CH₂Cl₂ (18 ml) was added to PCN-222(Pd). After warming the mixture to 33°C for 1 h, DPA-F₁₄@PCN-222(Pd) was collected by filtration and washed with CH₂Cl₂ (2×10 ml). From the supernatant solvent, the amount of DPA-F₁₄ absorbed was determined spectroscopically as 0.34 mg DPA-F₁₄ / mg PCN-222(Pd). The insertion of DPA-F₁₄ was substantiated by ¹⁹F MAS-NMR spectroscopy. ¹⁹F MAS-NMR: $\delta = -67.1, -121.8$ ppm.

d) Synthesis of CA@PCN-222(Pd)

After the removal of acetone by filtration, PCN-222(Pd) (15 mg, ca. 0.012 mmol) was dried under reduced pressure for 12 h at 60°C. Under an inert atmosphere, a solution of dry CA (10 ml) in dry toluene (20 ml) was added to PCN-222(Pd). After heating the mixture to 70°C for 1 h, CA@PCN-222(Pd) was collected by filtration and washed with CH₂Cl₂ (2×10 ml). IR spectroscopy confirmed the successful uptake.

In addition to the IR bands of the PCN-222(Pd) host, CA@PCN-222(Pd) displays IR bands of aliphatic CH oscillators (CH₂, CH₃) at 2953, 2922 and 2851 cm⁻¹ confirming the presence of CA (Figures S2, S8). The already broad band of the OH stretching vibration of neat CA (3300 – 2350 cm⁻¹) broadens significantly (3350 – 2000 cm⁻¹) in CA@PCN-222(Pd), suggesting the presence of additional hydrogen bonding interactions (Figures S2, S8). A sharp band at 2536 cm⁻¹ specific to CA@PCN-222(Pd) suggests distinct OH hydrogen bonds of CA with the MOF, likely the SBUs. The band of the C=O stretching vibration of CA (1705 cm⁻¹) splits into 1731 and 1685 cm⁻¹ pointing to coordinated and free C=O groups (Figures S2, S8). Bands at 1603 and 1566 cm⁻¹ can be assigned to carboxylates coordinating to Zr. Bands for C-O vibrations appear at 1275/1230 cm⁻¹. The

characteristic broad OH deformation band of hydrogen bonded CA dimers at 930 cm^{-1} (Figures S2, S8) diminishes in the MOF suggesting that only few CA molecules form such dimers in the channel.

e) Synthesis of CA/DPA@PCN-222(Pd)

After the removal of acetone by filtration, PCN-222(Pd) (15 mg, ca. 0.012 mmol) was dried under reduced pressure for 12 h at 60°C . Under an inert atmosphere, a mixture of DPA (30 mg, 0.09 mmol) and dry CA (10 ml) in dry toluene (20 ml) was added to PCN-222(Pd). After heating the mixture to 70°C for 1 h, CA/DPA@PCN-222(Pd) was collected by filtration and washed with CH_2Cl_2 (2×10 ml). From the supernatant solvent, the amount of DPA absorbed was determined spectroscopically.

Exemplary data:

sample	$T /$ $^\circ\text{C}$	PCN-222(Pd) / mg	DPA / mg	CA / ml	toluene / ml	uptake DPA / mg	ratio mg DPA / mg PCN
1	70	23	46	15	30	9.12	0.40
2	70	15	30	10	20	4.78	0.32
3	70	15	30	10	20	4.37	0.29
4	80	15	30	10	20	9.87	0.66

f) Release of DPA from CA/DPA@PCN-222(Pd) in toluene

DPA/CA@PCN-222(Pd) (15 mg with ca. 0.55 mg DPA / mg) was heated to 70°C in toluene (60 ml) for 5 h under an inert atmosphere. The amount of DPA released in toluene was determined by UV/Vis spectroscopy.

g) Release of DPA from CA/DPA@PCN-222(Pd) in water

DPA/CA@PCN-222(Pd) (15 mg with ca. 0.55 mg DPA / mg) was heated to 70°C in water (40 ml) for 2 h under an inert atmosphere. The amount of DPA released in water was determined by UV/Vis spectroscopy.

3. Spectroscopic Data

Figure S0. $^{13}\text{C}\{^1\text{H}\}$ NMR spectrum of Pd(TCPP) in DMSO- d_6 (* denotes residual solvent resonance).

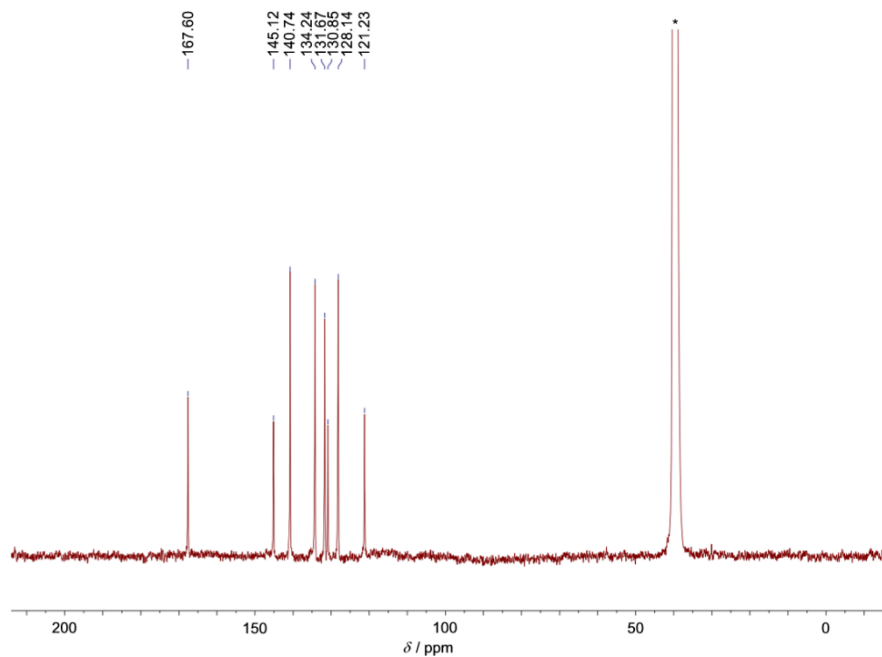


Figure S1. UV/Vis absorption and emission spectra of PCN-222(Pd); $\lambda_{\text{exc}} = 525$ nm.

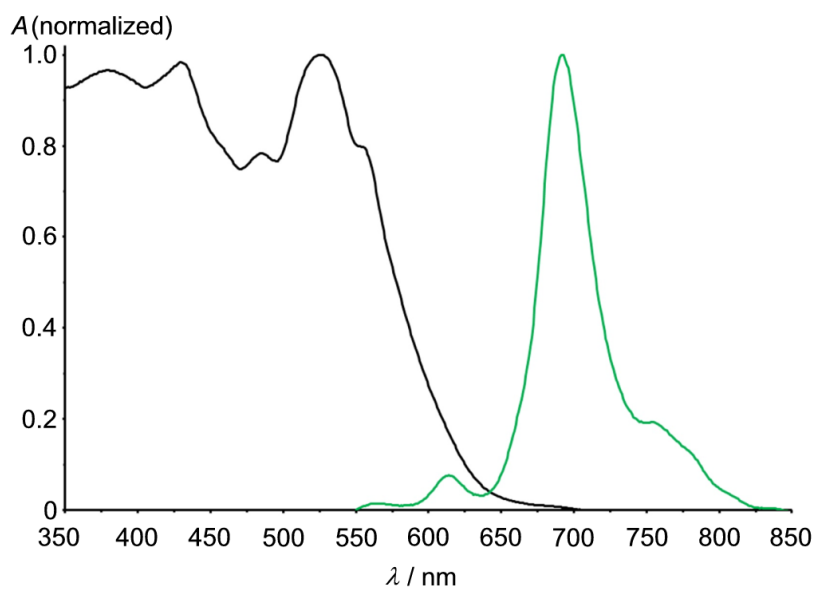


Figure S2. IR spectrum of PCN-222(Pd).

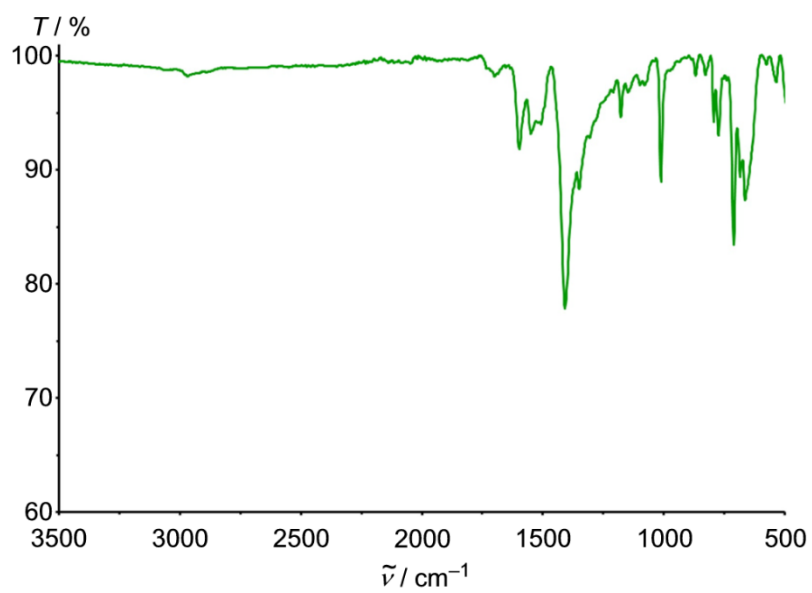


Figure S3. ^{19}F NMR spectrum of DPA-F₁₄ in CD_2Cl_2 .

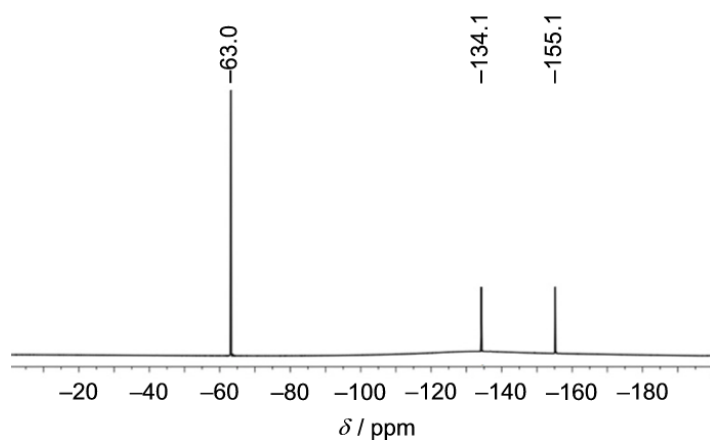


Figure S4. ^{19}F MAS NMR spectrum of DPA-F₁₄ (spinning frequency 20 kHz). Asterisks denote spinning side bands.

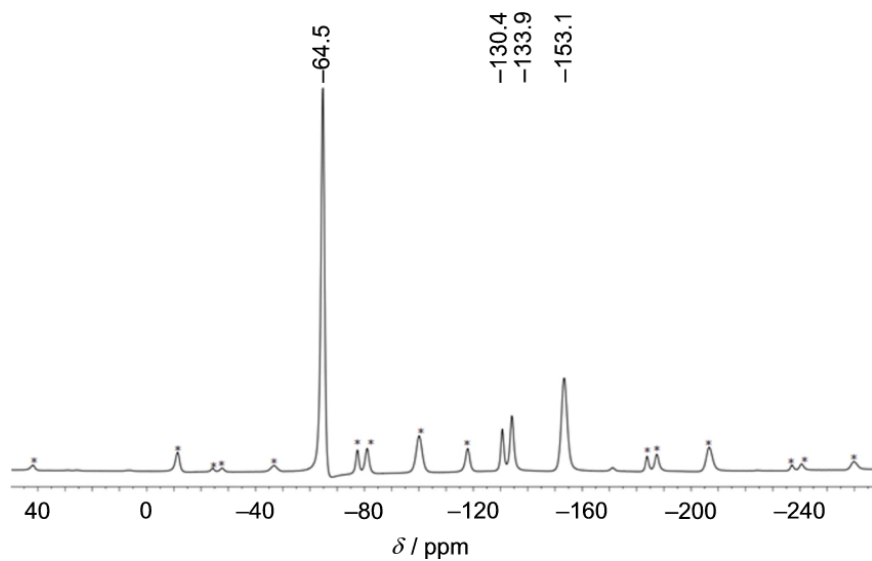


Figure S5. ^{19}F MAS NMR spectrum of DPA-F₁₄@PCN-222(Pd) (spinning frequency 20 kHz). The background is corrected by measuring the empty rotor considering the receiver gain and number of scans.

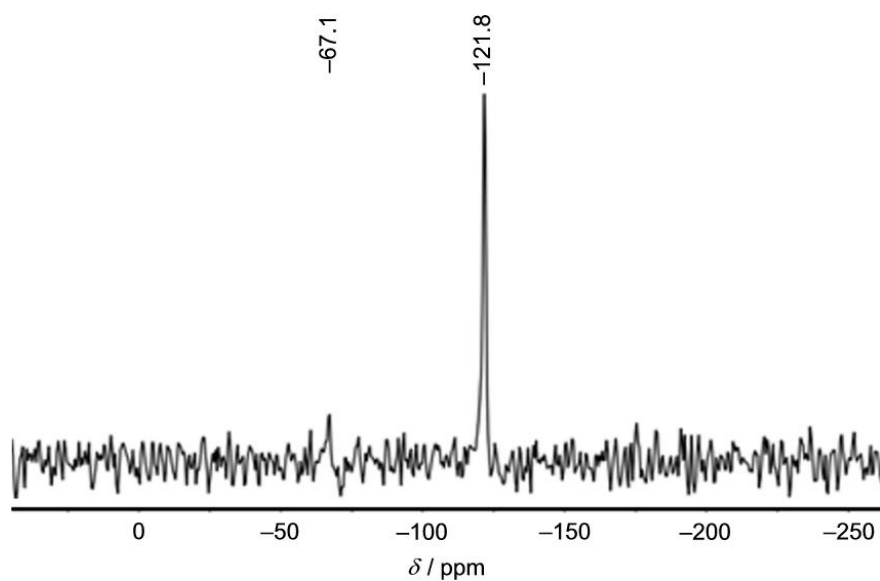


Figure S6. UV/Vis absorption (black) and emission spectra (blue) of DPA in toluene and emission spectrum (green) of DPA as solid; $\lambda_{\text{exc}} = 395$ nm. The green arrow indicates possible excimer emission of solid DPA.

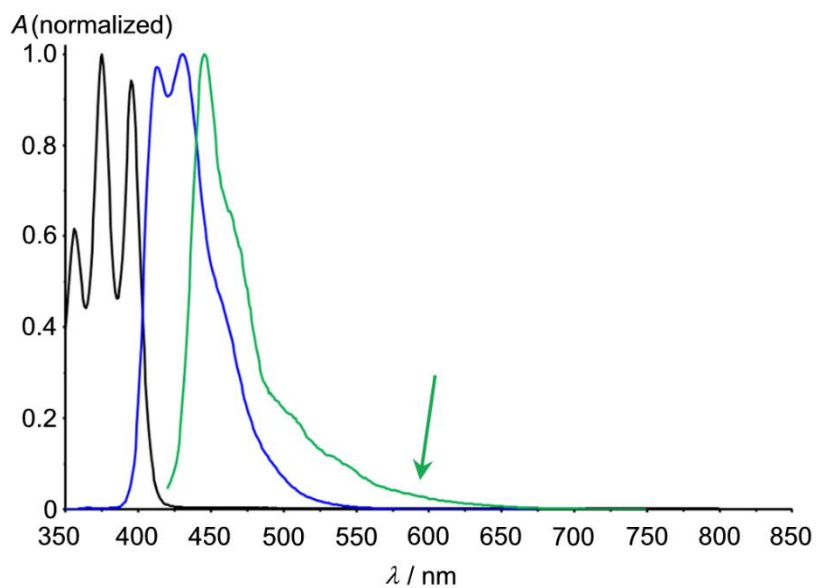


Figure S7. Experimental PXRD pattern of PCN-222(Pd) (red) and CA/DPA@PCN-222(Pd) (grey) and simulated PXRD pattern (black, fwhm $2\theta = 0.2^\circ$) of PCN-222(Pd).

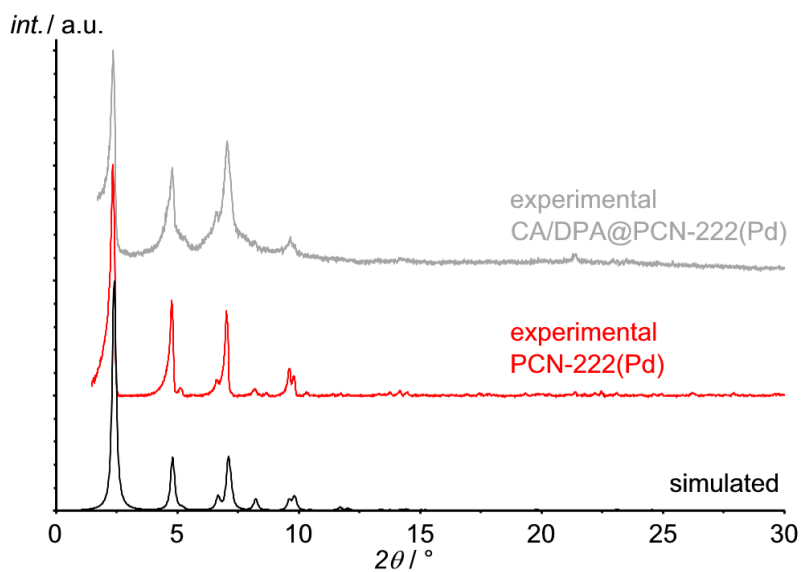


Figure S8. IR spectra of CA@PCN-222(Pd) (red) and CA/DPA@PCN-222(Pd) (blue).

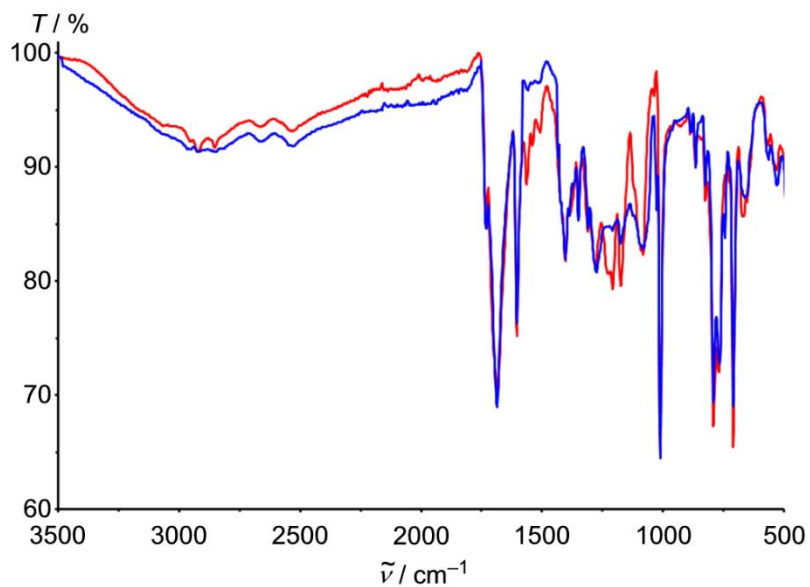


Figure S9. UV/Vis absorption spectra of PCN-222(Pd) (black) and CA/DPA@PCN-222(Pd) (blue) (normalized to the Q band at 556 nm). The characteristic UV absorption band of DPA at 397 nm is clearly visible.

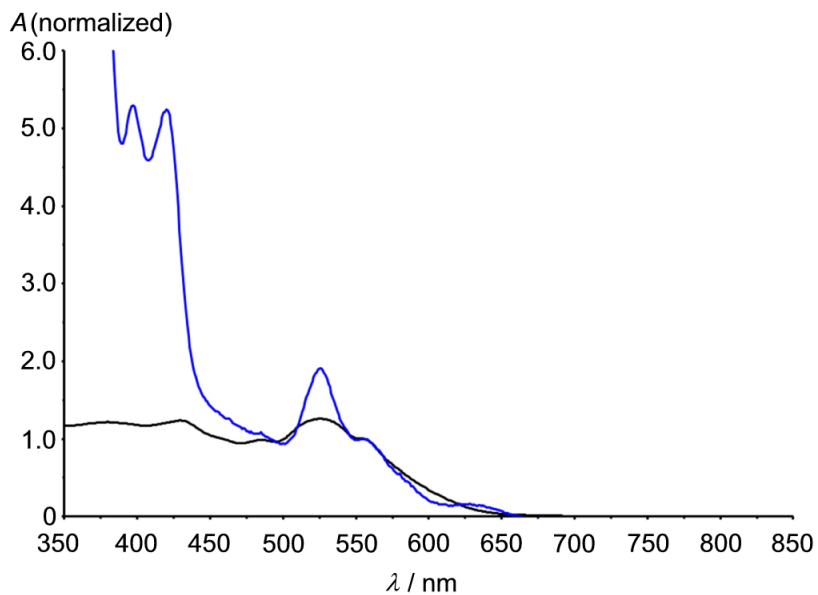


Figure S10. Stability of PCN-222(Pd) under laser irradiation ($\lambda_{\text{exc}} = 532 \text{ nm}$, 5.25 mW, 45 min) in the presence of O_2 traces. Photodegradation ceases after consumption of all O_2 .

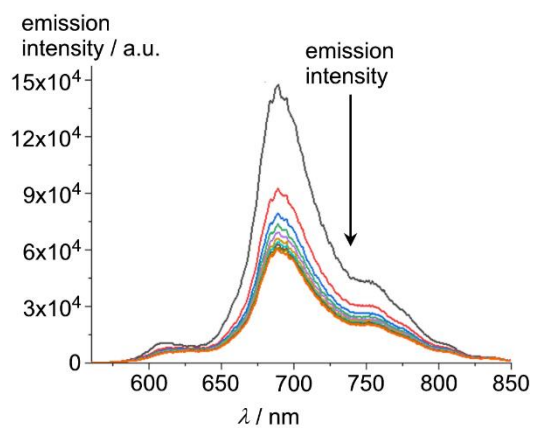


Figure S11. Stability of CA/DPA@PCN-222(Pd) under laser irradiation ($\lambda_{\text{exc}} = 532 \text{ nm}$, 5.25 mW, 45 min) in the absence of O_2 . Both the phosphorescence and the TTA-UC emission are stable.

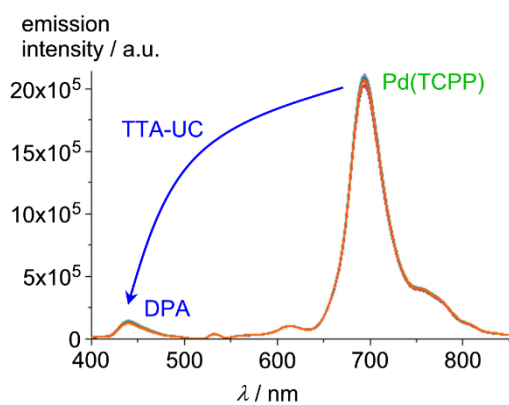


Figure S12. Fluorescence decay of DPA with $\lambda_{exc} = 410$ nm (determined on the FLS).

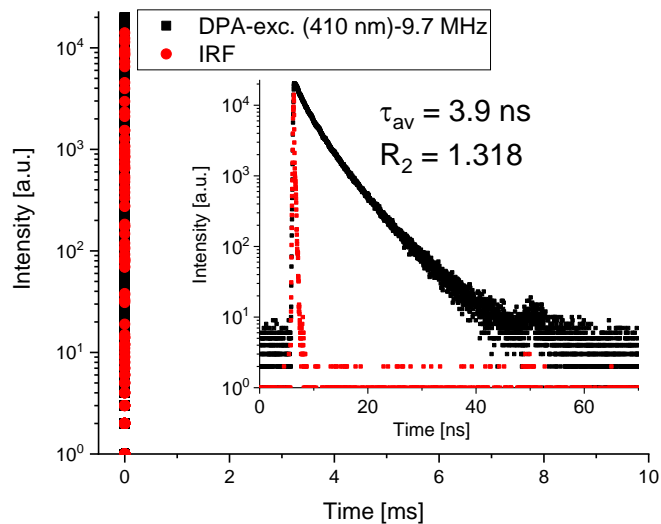


Figure S13. Fluorescence decay of DPA with $\lambda_{exc} = 405$ nm (determined on the fluorescence microscope).

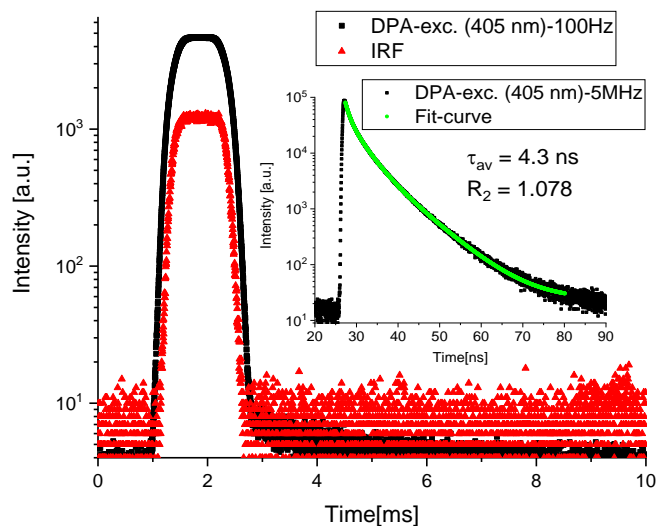


Figure S14. Luminescence decay of the DPA acceptor in CA/DPA@PCN-222(Pd) with $\lambda_{\text{exc}} = 524$ nm (determined on the fluorescence microscope).

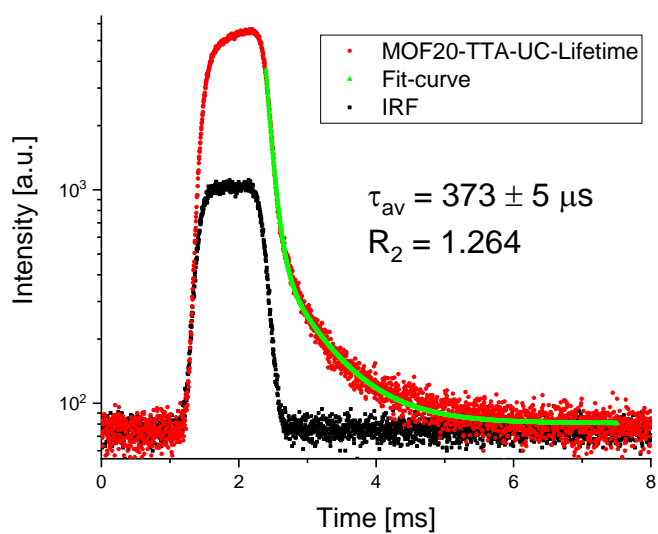


Figure S15. Luminescence decay of PCN-222(Pd) with $\lambda_{\text{exc}} = 524$ nm (determined on the fluorescence microscope).

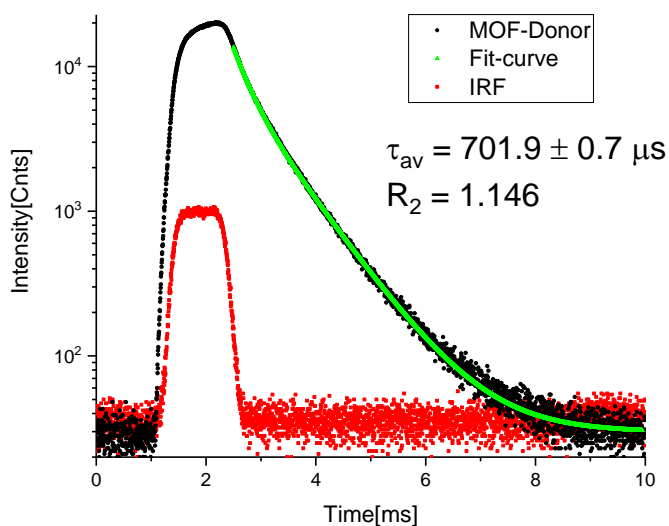


Figure S16. Luminescence decay of the donor in CA/DPA@PCN-222(Pd) with $\lambda_{\text{exc}} = 524 \text{ nm}$ (determined on the fluorescence microscope).

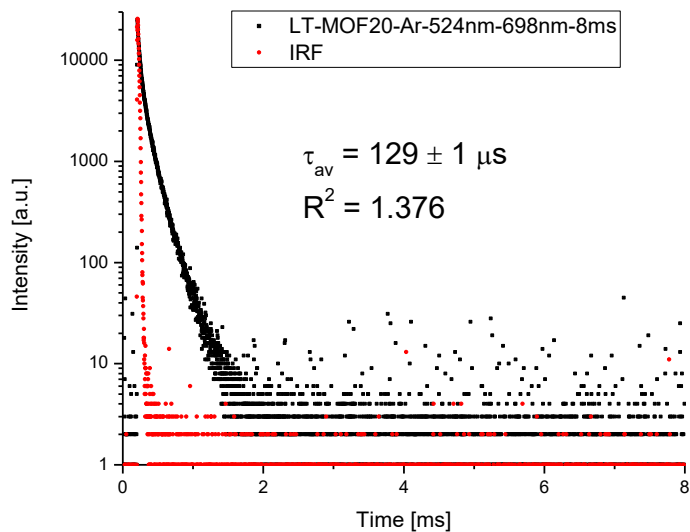


Figure S17. UCL emission of CA/DPA-PCN-222(Pd) under O_2 -free conditions (blue) and in the presence of O_2 (red).

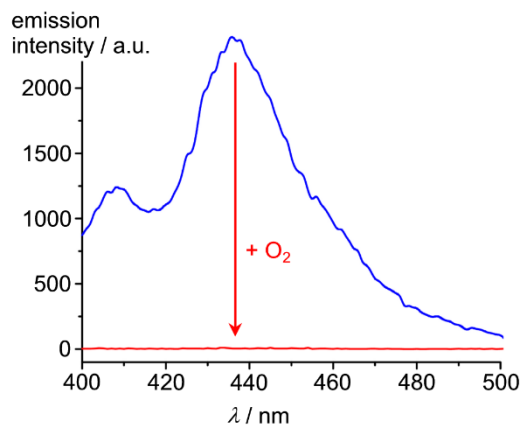


Figure S18. Emission spectra of PCN-222(Pd) (black) and UCL emission of CA/DPA-PCN-222(Pd) at three different points of the same sample (blue *).

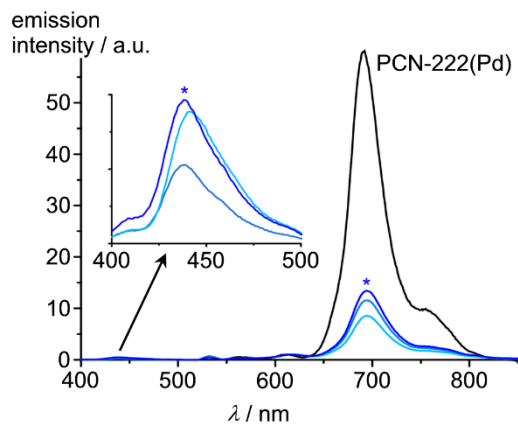


Fig S19. Optical photographs of solid CA/DPA-PCN-222(Pd) a) at ambient light, b) under laser irradiation (532 nm) with a short pass filter and c) under laser irradiation (532 nm) without a short pass filter.

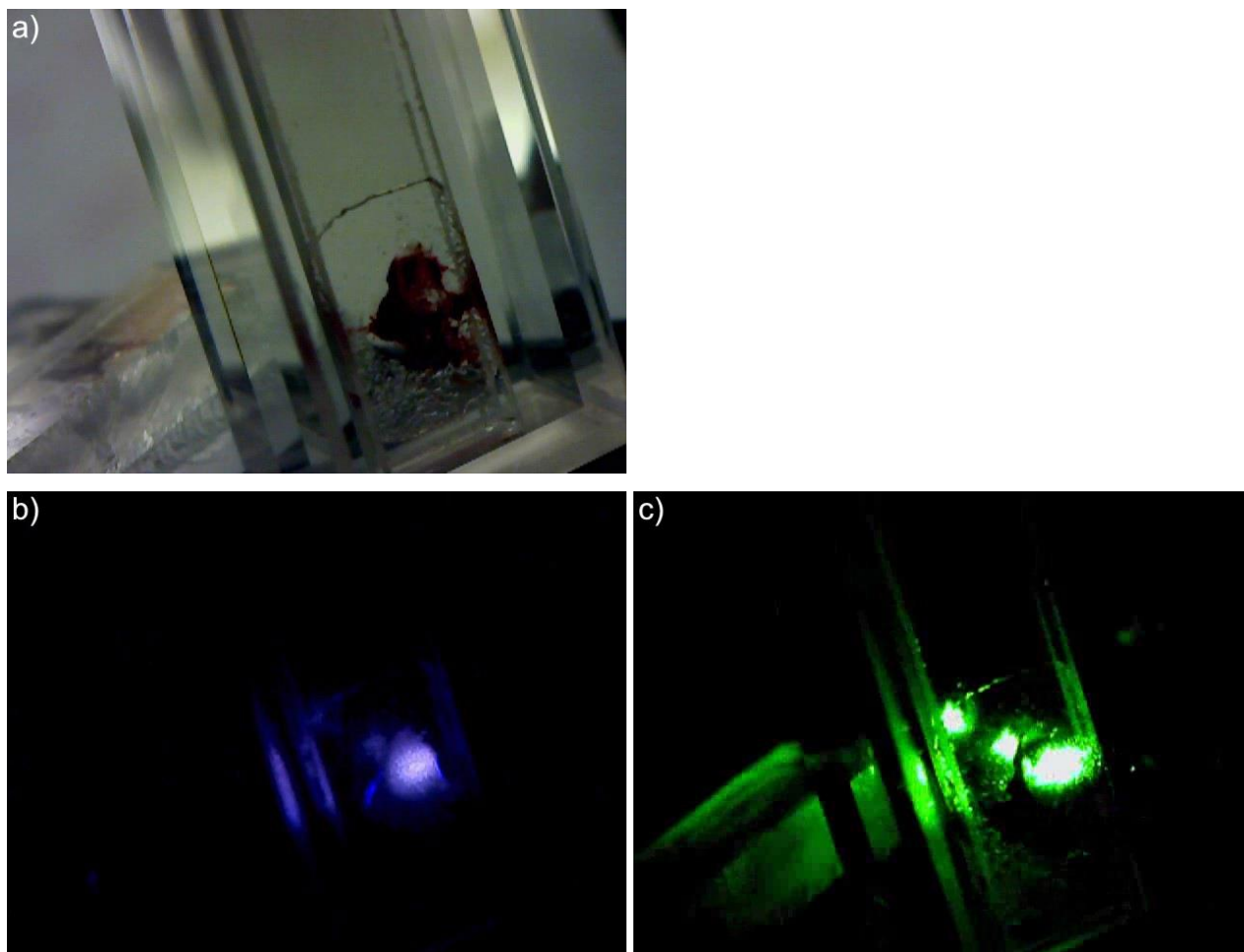
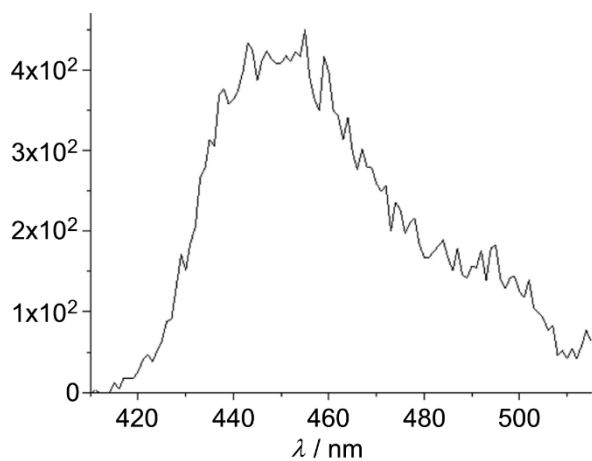


Figure S20. UCL emission of acceptor@PCN-222(Pd) with acceptor = 2,5,8,11-tetra-*tert*-butyl-perylene; $\lambda_{exc} = 532$ nm (conditions not optimized; some residual oxygen reduces the signal intensity, so that accumulation of more scans to reduce the S/N ratio is prohibited).

UCL intensity / a.u.



4. References

- 1 STOE & Cie, X.-R. X-Red, STOE & Cie, Darmstadt, Germany **2002**.
- 2 Mercury 3.5.1 (Build RC5), CCDC 2001–2014.
- 3 J. Chen, H. Chen, T. Wang, J. Li, J. Wang, X. Lu, *Anal. Chem.* **2019**, *91*, 4331–4336.
- 4 W.-P. To, Y. Liu, T.-C. Lau, C.-M. Che, *Chem. Eur. J.* **2013**, *19*, 5654–5664.
- 5 D. Feng, Z.-Y. Gu, J.-R. Li, H.-L. Jiang, Z. Wie, H.-C. Zhou, *Angew. Chem. Int. Ed.* **2012**, *51*, 10307–10310.